

Independently Tuning the Biochemical and Mechanical Properties of 3D Hyaluronan-Based Hydrogels with Oxime and Diels–Alder Chemistry to Culture Breast Cancer Spheroids

Alexander E. G. Baker,^{†,‡,§} Roger Y. Tam,^{†,‡} and Molly S. Shoichet^{*,†,‡,§}

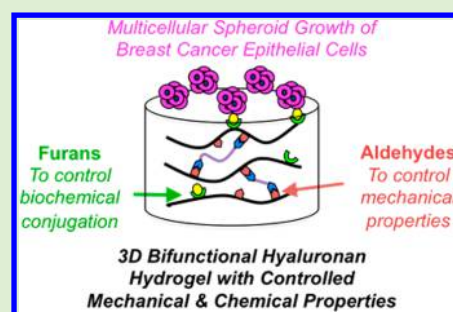
[†]Department of Chemical Engineering and Applied Chemistry, University of Toronto, 200 College Street, Toronto, Ontario M5S 3E5, Canada

[‡]Institute of Biomaterials and Biomedical Engineering, University of Toronto, 164 College Street, Room 407, Toronto, Ontario M5S 3G9, Canada

[§]Department of Chemistry, University of Toronto, 80 St. George Street, Toronto, Ontario M5S 3H6, Canada

Supporting Information

ABSTRACT: For native breast cancer cell growth to be mimicked in vitro as spheroids, a well-defined matrix that mimics the tumor microenvironment is required. Finding a biomimetic material for 3D cell culture other than Matrigel has challenged the field. Because hyaluronan is naturally abundant in the tumor microenvironment and can be chemically modified, we synthesized a hyaluronan (HA) hydrogel with independently tunable mechanical and chemical properties for 3D culture of breast cancer cells. By modifying HA with distinct bioorthogonal functional groups, its mechanical properties are controlled by chemical cross-linking via oxime ligation, and its biochemical properties are controlled by grafting bioactive peptides via Diels–Alder chemistry. A series of hydrogels were screened in terms of stiffness and peptide composition for cancer spheroid formation. In the optimal hydrogel formulation, the 3D breast cancer spheroids showed decreased drug diffusion into their core and upregulation of cellular multidrug-resistant efflux pumps similar to what is observed in drug-resistant tumors. Our results highlight the potential of these tunable and well-defined gels in drug screening assays.



INTRODUCTION

In vitro cell culture using three-dimensional (3D) scaffolds has emerged as a technique that can recapitulate in vivo cellular phenotypes and genotypes by providing cells with the necessary biochemical and mechanical cues.^{1–3} Differences between cells cultured on conventional 2-dimensional (2D) tissue culture polystyrene (TCPS) and in 3D scaffolds are extensive;^{4,5} for example, culture of breast epithelial cancer cells on 2D TCPS does not generate physiologically relevant multicellular spheroidal structures, whereas culture in the commercially available 3D scaffold, Matrigel, results in 3D breast cancer spheroids.^{3,6–8} Notwithstanding the benefits of cell culture in Matrigel, because it is extracted from Engelbreth–Holm–Swarm (EHS) mouse sarcoma, it has an ill-defined composition that often results in irreproducible data, batch-sensitive drug screening results, and consequently an unclear mechanistic understanding.^{9–11} In addition, the use of Matrigel alone can not be formulated to study the independent effects of mechanical and biochemical properties, that is, gel stiffness and immobilized bioactive molecules, respectively, which are important extracellular matrix parameters that significantly affect cellular behavior.^{8,12}

Compositionally defined 3D hydrogel scaffolds comprising naturally derived or synthetic polymers are advantageous for cell culture, overcoming the inherent limitations of both

conventional 2D cell culture and 3D culture in the naturally derived but ill-defined Matrigel.^{13–15} Hyaluronan (HA) is a nonsulfated glycosaminoglycan that is particularly interesting for 3D culture as it is both abundant and upregulated in numerous tumor tissues and plays a significant role in tumor metastasis.^{16–18} Because of its biological relevance for tumor growth, and that many cancer cells express CD44 (a cell-surface receptor for HA), HA-based hydrogels have been explored as tools to study oncogenesis.^{19,20}

The chemical and mechanical properties of the cellular microenvironment influence cell fate,^{21,22} and these properties must be considered in the design of hydrogels for cancer cell culture. Several strategies have been pursued to immobilize bioactive ligands and covalently cross-link HA to form stable 3D scaffolds for cell culture.^{13,23} Acrylate-thiol Michael addition click chemistry, such as that used in HyStem,²⁴ is a prevalent reaction and can be used to immobilize bioactive ligands, but this inherently limits independent control of cross-linking and chemical ligand presentation as both cross-linkers and ligands compete for the same thiol groups on the HA backbone.

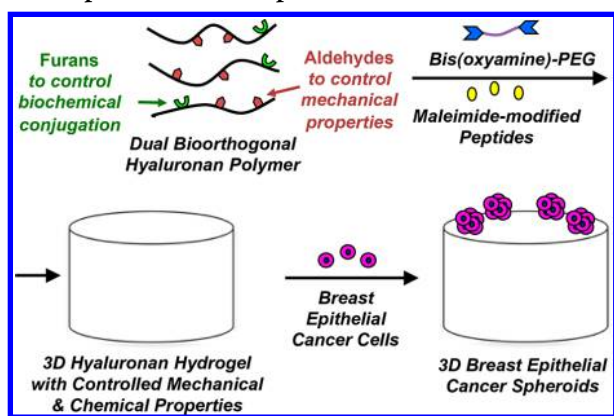
To enable independent control of mechanical and biochemical parameters, we designed a defined HA hydrogel that

Received: October 2, 2017

Published: October 17, 2017

takes advantage of two bioorthogonal chemical strategies (i.e., oxime ligation and Diels–Alder reaction) within the same HA polymer backbone. Specifically, HA polymers were first modified with aldehyde groups and then with methyl furan motifs. The HA-aldehyde groups are cross-linked with bis(oxyamine)-poly(ethylene glycol) (PEG) via oxime ligation to control hydrogel mechanical properties, whereas the HA-methylfuran groups are conjugated with maleimide-functionalized bioactive peptides via Diels–Alder reaction to control hydrogel biochemical properties.^{25,26} Thus, this hydrogel system, comprising dual click chemistries on the same polymeric backbone, allows for distinct modulation of mechanical stiffness through cross-linking and bioactivity through chemical functionalization (Scheme 1) and is advanta-

Scheme 1. Biomimetic Bifunctional Hyaluronan-Based Hydrogels with Independently Controlled Mechanical and Chemical Properties and Their Application in Culturing Breast Epithelial Cancer Spheroids



geous over using the combination of two separate monofunctionalized polymers. We demonstrate how both mechanical and biochemical properties of the hydrogel influence the formation of 3D breast cancer spheroids and identify the optimal combination. We then examine the potential utility of these defined hydrogels for in vitro drug screening (Scheme 1).

EXPERIMENTAL SECTION

Materials. All chemical reagents were used directly as provided by the suppliers unless otherwise stated. All materials were purchased from Sigma-Aldrich unless indicated otherwise: sodium hyaluronate (289 kDa, Lifecore Biomedical), aminoacetaldehyde dimethyl acetal, 5-methyl-2-furanmethanamine (TCI), 4-(4,6-dimethoxy-1,3,5-triazin-2-yl)-4-methylmorpholinium chloride (DMT-MM), poly(ethylene glycol) bis-amine (number-average molar mass (M_n) 3400 g/mol, Shearwater), (boc-aminoxy)acetic acid, *N,N*-diisopropylcarbodiimide, *N,N*-diisopropylethylamine, 3-maleimidopropionic acid (TRC), triisopropylsilane, *N* α -Fmoc-*N* ϵ -Alloc-*L*-lysine (Anaspec), phenylsilane, acetic anhydride, palladium-tetrakis(triphenyl phosphine), *O*-(6-chlorobenzotriazol-1-yl)-*N,N,N',N'*-tetramethyluronium hexafluorophosphate (Anaspec), methyl cellulose dialysis membrane (1000 Da and 12–14 kDa cutoff), growth-factor reduced Matrigel (Corning product # 354230, lot # 4041123), HyStem C (Sigma-Aldrich product #HYS010-1KT), 2-(*N*-morpholino)-ethanesulfonic acid (MES) (Bio Basic Canada Inc.), Dulbecco's phosphate buffered saline, Dulbecco's modified Eagle's medium without sodium bicarbonate, RPMI-1640 medium (product # R8758), Dulbecco's modified Eagle's medium/Nutrient F-12 Ham (product # D6421), trypsin EDTA (product # T4049), charcoal-filtered fetal bovine serum (product # 12483-020) (Gibco), collagen IV (product # 356233) (Corning), 0.4% trypan blue (product # T8154), Hoechst 33342 (product # H1399) (Invitrogen),

Alexafluor 488 Phalloidin (product # A-12379) (Molecular Probes), EasiVial PEG (Part # PL2080-0201, Lot # 0006156930), and hyaluronidase from bovine testes, type IV-S (H3884).

Dimethoxy Acetal-Substituted Hyaluronan (HA-dma) (1). Sodium hyaluronate (for 51% degree of substitution (D.S.): 0.5 g; for 68% D.S.: 1.0 g, 289 kDa) was dissolved in 0.1 M MES buffer (8.3 mL/g of sodium hyaluronate, pH 5.5) and mixed with DMT-MM (for 51% D.S.: 0.55 g, 1.98 mmol; for 68% D.S.: 1.17 g, 4.22 mmol). The reaction was stirred for 15 min, and aminoacetaldehyde dimethyl acetal (for 51% D.S.: 0.14 g, 1.31 mmol; for 68% D.S.: 0.50 g, 4.75 mmol) was added. After stirring for 48 h at room temperature, the solution was dialyzed extensively in 0.1 M NaCl (5 times, 12–14 kDa molecular weight cutoff), followed by distilled water (3 times). The purified solution was lyophilized and analyzed by ¹H NMR (Figure S1) in deuterium oxide (D₂O) to determine dimethoxy acetal substitution of 51% (1a) or 68% (1b).

Methyl Furan/Dimethoxy Acetal-Substituted Hyaluronan (HA-MF-dma) (2). Dimethoxy acetal-substituted hyaluronan (1a or 1b) (0.22 g, 289 kDa) was dissolved in 0.1 M MES buffer (26 mL, pH 5.5) and mixed with DMT-MM (0.147 g, 0.53 mmol). The reaction was stirred for 15 min, and 5-furfurylamine (59 mg, 0.53 mmol) was added dropwise. After stirring for 24 h at room temperature, the solution was dialyzed against 0.1 M NaCl and then distilled water (3 times). The purified solution was lyophilized, resulting in 2a or 2b (0.21 g, 93% yield), and was analyzed by ¹H NMR in D₂O to determine methyl furan substitution of 16% (Figure S2).

Methylfuran/Aldehyde-Substituted Hyaluronan (HA-MF-Ald) (3). Methylfuran/dimethoxy acetal-substituted hyaluronan (2a or 2b) (211 mg, 289 kDa) was dissolved in distilled water (10 mL) and dialyzed in 0.2 M HCl (12–14 kDa molecular weight cutoff) for 48 h at room temperature followed by distilled water for 24 h. The purified solution was lyophilized, resulting in 3a or 3b (0.165 g, 87% yield), and ¹H NMR was used to monitor the completion of the reaction via the disappearance of acetal signal at 3.45 ppm (Figure S3). Gas permeation chromatography was used to investigate the change in molecular weight of unmodified HA to HA-MF-ald by comparison to poly(ethylene glycol) (PEG) standards and revealed a decrease in molecular weight from M_w 330.1 to 284.1 kg mol⁻¹.

Quantification of Aldehyde Substitution in the HA Polymer Backbone for Compounds. Aldehyde substitution was quantified as previously reported.²⁷ Briefly, aldehyde-substituted hyaluronan (10 mg) (3a, 3b, or 7) was dissolved in acetate buffer (0.75 mL, 0.1 M in water, pH 5.2), mixed with a solution of *tert*-butyl carbazate (15.6 mg, 0.12 mmol) and sodium cyanoborohydride (7 mg, 0.12 mmol) in acetate buffer (0.75 mL), and stirred for 24 h at room temperature. The solution was sequentially dialyzed against 0.1 M NaCl and distilled water and lyophilized to afford HA-hydrazide (Boc) derivatives (4a, 4b, 8 corresponding to 3a, 3b, 7, respectively). ¹H NMR was used to determine aldehyde substitution by the ratio of integrals corresponding to *tert*-butyl (1.47 ppm) and *N*-acetamide (2.03 ppm) (Figures S4, S5, and S8).

Poly(ethylene glycol) Bis(oxyamine) (5). To a solution of dichloromethane (DCM) (3 mL) under nitrogen were added (boc-aminoxy)acetic acid (0.035 g, 0.18 mmol) and *N,N'*-diisopropylcarbodiimide (DIC) (0.033 g, 0.26 mmol), which was then stirred for 1 h at 0 °C. PEG diamine (0.300 g, 3400 MW) was added with *N,N*-diisopropylethylamine (0.022 g, 0.18 mmol), and the reaction was stirred for 48 h at room temperature. Completion of the PEG modification reaction was confirmed using ¹H NMR by the disappearance of the terminal methylene ($-CH_2-NH_2$) signals at 3.0 ppm (Figure S4) and the appearance of the *tert*-butyl groups (1.5 ppm) of the Boc-protected bis(oxyamine). DCM was evaporated under reduced pressure. The resulting solid was dissolved in a mixture of 0.1 M MES buffer (pH 5.5) and dimethylformamide (DMF) and then dialyzed using a methyl cellulose dialysis membrane (1000 Da molecular weight cutoff) in sodium chloride (0.1 M) followed by distilled water (3 times) before being lyophilized. Boc-protected PEG bis(oxyamine) (5a) was obtained as a white solid (268 mg, 79% yield) and characterized for substitution by ¹H NMR. Boc groups were cleaved by dialysis in hydrochloric acid (0.2 M) followed by DI water.

PEG bis(oxyamine) (5) was obtained as a white crystalline solid (200 mg, 82% yield) and characterized by ^1H NMR (Figure S6).

Mal-IKVAV-L₆ Peptide. Mal-GRKQAASIKVAVSG₄SRL₆-R₂KG was prepared using Fmoc-Glycine-Wang Resin and standard Fmoc solid phase synthesis. Following piperidine deprotection of the *N*-terminus, maleimide functionality was immobilized by activating 3-maleimido-propionic acid (84 mg, 0.5 mmol) with DIC (0.120 mL, 0.75 mmol) in DCM (6 mL) and 1-methyl-2-pyrrolidinone (0.2 mL) for 30 min. The solution was added to preswollen resin-containing peptide (0.25 mmol) in DCM and stirred overnight. Peptides were cleaved off the resin using 90% trifluoroacetic acid, 5% water, and 5% triisopropylsilane over 4 h at room temperature. The crude peptide was precipitated into cold ether and purified by HPLC with water and acetonitrile containing 0.1% trifluoroacetic acid. ESI calcd for C₁₃₆H₂₄₂N₄₆O₃₇ [M]⁺, 3112.85; found, 3112.9.

Mal-YIGSR-L₆ Peptide. Mal-GDPGYIGSRG₄RL₆R₂KG was prepared using the above protocol for peptide synthesis. ESI calcd for C₁₁₆H₁₉₅N₃₈O₃₂ [M + NH₄]⁺, 2649.51; found, 2647.5.

RGD-L₆-Mal Peptide. Ac-GRGDSPASSKG₄SRL₆R₂KK(Mal)G was prepared using the above solid phase synthesis protocol with the following modifications: Fmoc-Glycine-Wang resin (1.0 mmol) first coupled to *N*α-Fmoc-*N*ε-Alloc-*L*-lysine (0.68 g, 1.5 mmol) using HCTU (0.78 g, 1.88 mmol) and DIPEA (0.37 mL, 2.25 mmol) overnight. Subsequent Fmoc deprotections of the *N*-termini were achieved using 20% piperidine in DMF containing 0.1% HOBT. Following cleavage of the final Fmoc residue, the peptide was *N*-capped using acetic anhydride (0.2 mL) and DIPEA (0.5 mL) in DCM for 2 h. Completion of reactions were monitored using a 2,4,6-trinitrobenzenesulfonic acid (TNBS) test. Alloc deprotection was performed in DCM under nitrogen with palladium-tetrakis(triphenyl phosphine) (catalytic) and phenylsilane (0.31 mL, 2.5 mmol) overnight. C-terminal maleimide functionalization was performed by activating 3-maleimido-propionic acid (253 mg, 1.5 mmol) with DIC (0.70 mL, 2.25 mmol) in DCM (6 mL) and 1-methyl-2-pyrrolidinone (0.2 mL) for 30 min. The solution was added to preswollen resin in DCM and stirred overnight. Peptides were purified as above. ESI calcd for C₁₂₅H₂₁₈N₄₃O₃₈ [M + H]⁺, 2930.64; found, 2930.68.

Preparation of Bifunctional Hyaluronan Hydrogels. Sterile HA polymer (25 mg mL⁻¹ in Dulbecco's modified Eagle's medium without sodium bicarbonate) was diluted to the desired concentration with Dulbecco's phosphate buffered saline (DPBS) and transferred into each of the desired wells. Sterile poly(ethylene glycol) bis(oxyamine) solution (72 mg mL⁻¹ in 0.1 M phosphate buffer pH 7.4) was then added to each well and immediately, yet carefully to avoid air bubbles, mixed with a pipet. Increased gel viscosity was observed within 5 s. Completion of gelation was achieved by incubation for 45 min at 37 °C in 5% CO₂. The hydrogels were washed with DPBS (once) followed by 0.1 M MES buffer (pH 5.5, 2 times). Scaffolds were modified by incubation with the desired concentration of maleimide-modified peptides (dissolved in 10% DMSO in 0.1 M MES pH 5.5) overnight at 37 °C. Hydrogels were washed twice with MES (30 min each), twice with 0.3 M glycine solution (diluted in PBS), and twice with phosphate buffer (0.1 M, pH 8).

Preparation of Matrigel Hydrogels. Growth factor-reduced Matrigel was allowed to reach 4 °C over several hours, and using prechilled tips, the appropriate volume was transferred to the desired wells.

Preparation of HyStem Hydrogels. 3D HyStem hydrogels were prepared according to manufacturer's protocols and based on the reported procedure.²⁸

Hydrogel Swelling. Hydrogels were prepared (100 μL/gel) and incubated for 2 h at 37 °C to ensure full gelation. The hydrogel mass was taken as the nonswollen value, and DPBS (400 μL) was added to the hydrogels, which were incubated at 37 °C. Every 24 h, buffer was removed, and hydrogel mass was recorded and replaced with DPBS (400 μL) until hydrogel degraded over 28 days. Swelling data was recorded as a ratio of initial gel mass at a specific day to nonswollen hydrogel mass.

Unconfined Mechanical Testing to Determine Compressive Moduli. First, 75 μL of each gel was prepared in 16-well chamber slides with a surface area of 0.4 cm². Gels were washed and preswollen in PBS for 24 h prior to analysis. Samples were placed between two impermeable flat platens connected to a single axis load cell (150g, ATI Industrial Automation) on a Mach-1 micromechanical system (Biomomentum), and an initial force of 0.01 N was applied find the gel surface. The initial sample height was determined as the separation distance between the two platens. An initial uniaxial, unconfined compression was applied at a strain of 10% of the gel height to remove surface defects. Sample analysis was performed by applying a subsequent strain of 10%. The compressive modulus was calculated from the slope of the resultant stress versus strain chart for each sample. At least 3 separate samples were prepared and analyzed for each condition.

Quantification of Peptide Immobilization to HA Hydrogels by Amino Acid Analysis. HA-MF-ald hydrogels (100 μL) were formulated with 11 mg mL⁻¹ HA-MF-ald substituted with aldehyde (51%) and methyl furan (16%) cross-linked with 5.8 mg mL⁻¹ of 3.5 kDa PEG bis(oxyamine) for low PEG cross-linked (25% cross-linking) or 17.4 mg mL⁻¹ of PEG bis(oxyamine) for high PEG cross-linked (75% cross-linking) in PBS, which were prepared and incubated for 1 h at 37 °C. Hydrogels were washed twice with 0.1 M MES buffer (pH 5.5) for 10 min each followed by the respective addition of maleimide-modified IKVAV-L₆, YIGSR-L₆, or RGD-L₆ solutions (100 μL, 161 μM) in MES with 5% DMSO. Gels with a higher concentration of IKVAV-L₆ were prepared by the addition of 100 μL (805 μM peptide in MES with 5% DMSO). The hydrogels were incubated overnight at 37 °C and washed with MES, 0.1 M aminoxyacetic acid (in PBS), and PBS before being degraded by treatment with 5U of type IV hyaluronidase (5.55 μL) and incubated for another 48 h at 37 °C until completely digested. Samples were compared to controls containing only hyaluronan hydrogel + hyaluronidase spiked with an equal amount of maleimide-modified peptide solutions used for immobilization. Samples containing peptides are hydrolyzed to individual amino acids using 6 N HCl at 110 °C for 24 h. Excess HCl was removed by evaporation under reduced pressure, and the hydrolyzed amino acids were derivatized using phenylisothiocyanate (PITC). The phenyl-labeled amino acids were then separated, and samples were quantified using Pierce amino acid standard H and an Acquity UPLC BEH C18 column (2.1 mm X 10 cm) at 48 °C. Signal was detected at 254 nm using an Acquity TUV detector; results were processed using Waters Empower 2 chromatography software, and glycine values were used for analysis with *n* = 3 gels per condition. To calculate the conjugation efficiency of maleimide-modified peptides immobilized into a hydrogel sample, we compared the amount of immobilized peptides to standard solutions with known concentrations of HA-MF-ald and maleimide-modified peptides.

Quantification of Bis(oxyamine)-PEG Immobilization to Bifunctional Hyaluronan Hydrogels. Bifunctional HA hydrogels (51% aldehyde D.S.) cross-linked with bis(oxyamine)-PEG (3.5 kDa (75 repeating ethylene glycol units), 100% molar ratio oxyamine_{PEG}:aldehyde_{HA}) were prepared in D₂O/DMSO-*d*₆ (3:1 v/v). Hydrogels were washed with D₂O/DMSO-*d*₆ to remove unbound reagents. Hyaluronidase (5 U in 5.55 μL) was added to degrade the gels for 24 h at 37 °C. The degraded gel was then lyophilized and resuspended in D₂O/DMSO-*d*₆ for ^1H NMR acquisition. As a standard, the pyranose proton peaks (3.3–4.1 ppm, 10H) of HA-MF-ald alone (Figure S9B) were first quantified relative the C2-NHAc peak (2.1 ppm, 3H). For the conjugation efficiency of bis(oxyamine)-PEG immobilized within the HA gels, peaks between 3.3 and 4.1 ppm (corresponding to the methylene peaks of PEG and the pyranose peaks of HA-MF-ald) were integrated relative to the C2-NHAc peak of HA-MF-ald (Figure S9C) and compared to the theoretical amount of bis(oxyamine)-PEG initially added: theoretical number of PEG protons per mol_{HA} = (100% mol_{oxyamine added}/mol_{aldehyde DS on HA}) × (51% aldehyde_{DS on HA}/mol_{HA}) × (1 mol_{PEG added}/2 mol_{oxyamine added}) × ((75 repeating units/mol_{PEG}) × (4 H_{3.3–4.1 ppm/repeating unit}) + 4 terminal H_{3.3–4.1 ppm/mol_{PEG}} + 4 αH_{3.3–4.1 ppm/mol_{cross-linked PEG}}).

Cell Seeding. Cells were cultured using DMEM/F12 (MCF-7) or RPMI-1640 (T47D) supplemented with penicillin-streptomycin (1%), fetal bovine serum (10%), and insulin (0.01 mg/mL). Cells were passaged by removing media and rinsing the cells with PBS before adding trypsin EDTA (3 mL). Gels were equilibrated with media by washing 3 times prior to cell seeding. Then, 45 μL of gel/well was prepared in 96-well plates. Cells were diluted to the desired concentration using media, and 100 μL of cell solution was added to each well (i.e., for 6,000 cells/well, 100 μL of 60,000 cells/mL was added). For cells cultured on Matrigel, preformed Matrigel gels of 100% (8–12 mg mL⁻¹) were seeded on the surface with cells suspended in a media solution containing dilute 2.5% Matrigel as previously described.²⁹ For cells cultured on bifunctional-HA hydrogels, preformed HA-MF-ald gels were seeded on the surface with cells suspended in media followed by additional media containing IKVAV-L₆ (20 μM) and YIGSR-L₆ (1 μM) peptides and the addition of collagen IV (20 μg mL⁻¹). With the added proteins and peptides, we were able to eliminate all use of ill-defined Matrigel in our well-defined HA-MF-ald cell studies. Media was changed every 48 h, and gels with cells were maintained at 37 °C in 5% CO₂.

Quantification of Spheroid Number and Size. Spheroid size was quantified using a GelCount instrument without further treatment at 2400 dpi with settings as follows. Edge detection (65), dark on light detection mode, center detection sensitivity (60), colony intensity (0.1–0.5), circularity factor (60), number of spokes (12), fast Gaussian fit (3), good edge factor (80), and overlap threshold (50). In some wells, the colony intensity was adjusted to eliminate background by adjusting the colony intensity threshold. Spheroid diameters were binned and graphed using GraphPad.

Treatment with Doxorubicin. Fresh drug solutions were prepared from a 5 mM stock of doxorubicin prepared in DMSO and stored at –80 °C. Drug solutions at 10 nM, 50 nM, 100 nM, 1 μM , and 10 μM were prepared by serial dilution with RPMI-1640 media containing 10% fetal bovine serum and penicillin-streptomycin. A control solution containing 0.2% of DMSO was prepared from DMSO in the same media. Seven days after initially seeding cells, media were carefully removed from the wells and the cells were dosed with 150 μL of drug solution. The media was replenished with fresh drug solutions every 48 h. For visualizing the penetration of doxorubicin into cancer spheroids, seven days after seeding 6,000 T47D cells per well in a 96-well plate, media were carefully removed from the wells and cells were dosed with 150 μL of 10 μM of a doxorubicin solution. After 7 days of drug treatment, Hoechst 33342 (1/1000 dilution in media) was added to each well. After incubating the cells for 4 h at 37 °C, cancer spheroids were imaged at 20 \times magnification using an inverted confocal microscope to capture z-stack images with 10 μm step sizes.

Immunocytochemistry. Media were carefully removed using a pipet, and 50 μL of 4% PFA (dissolved in PBS) was added at room temperature (15 min for 2D culture and 1.5 h for 3D gels). Gels were then carefully washed with 75 μL of PBS (4 times, 20 min each with gentle agitation), and 2% BSA in PBS containing 0.1% TritonX was used to block nonspecific interactions for at least 1 h. Primary antibody (1/100 dilution for rabbit-MDR1 (anti-P glycoprotein antibody [EPR10364-57], Abcam, ab170904) or 1/100 dilution for Phalloidin-AlexaFluor488 (ThermoFisher, A12379) were diluted in 2% BSA/PBS containing 0.1% TritonX, and 20 μL was added to each well and incubated at 4 °C overnight with gentle agitation. Gels were then washed extensively with 2% BSA/PBS containing 0.1% TritonX with gentle agitation (5 times, at least 1 h each time). For MDRI, secondary antibodies (goat antirabbit-AlexaFluor 488, 1/100 dilution) and Hoechst (1/1000 dilutions) were diluted into the same solution in 2% BSA/PBS containing 0.1% TritonX and filtered through a 0.2 μm syringe filter. Twenty microliters was added to each well and incubated at room temperature for 2 h with gentle agitation. Gels were then washed using 2% BSA/PBS containing 0.1% Triton X extensively (5 times, at least 1 h each time with gentle agitation).

Cell Imaging. Cells were imaged using an Olympus Fluoview (FV1000) inverted confocal microscope. Images were taken with a 20 \times objective lens and acquired as Z-stacks (with 10 μm step size)

that spanned the entire 3D volume of the regions. All images for the same experiment were acquired using the same microscope settings, processed using the same software settings on FV10-ASW3.1, and displayed as compressed z-stacks. The same microscope settings were used for each set of experiments. Negative controls were performed using cells stained only with secondary antibodies.

Statistical Analysis. All statistical analyses were performed using GraphPad Prism version 6.00 for Mac (GraphPad Software, San Diego, CA, USA). For frequency distribution of spheroid sizes, sizes were binned at 50 μm , and a polynomial line of best fit is shown for clarity. Differences among groups of three or more treatments were assessed by one- or two-way ANOVA with Tukey post hoc tests to identify statistical differences. An α level of 0.05 was set as the criterion for statistical significance. Graphs are annotated with *p*-values represented as **p* ≤ 0.05, ***p* ≤ 0.01, ****p* ≤ 0.001, and *****p* ≤ 0.0001. All data are presented as mean + standard deviation.

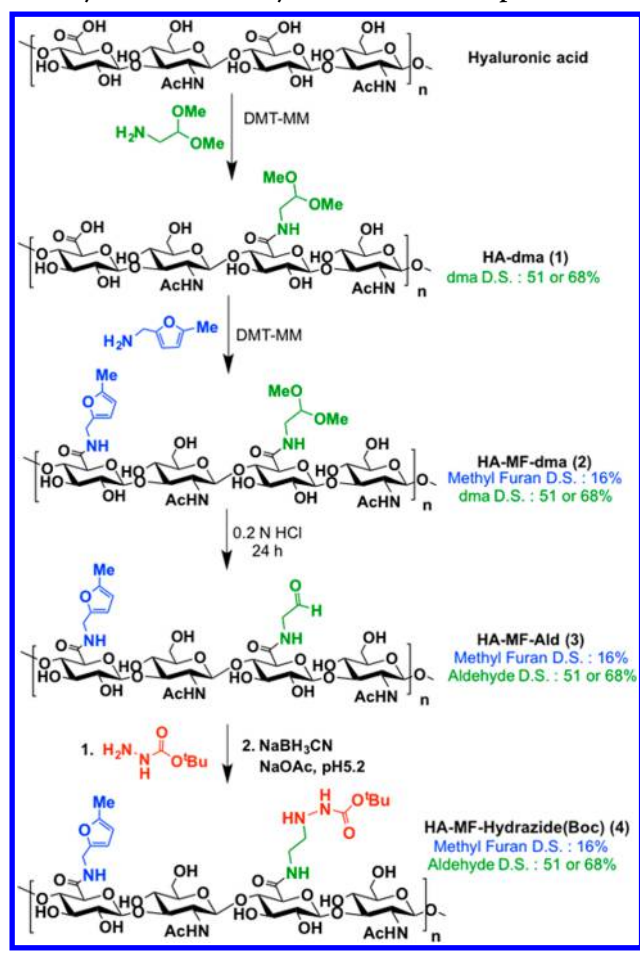
RESULTS AND DISCUSSION

To control hydrogel mechanical properties, we used oxime chemistry to chemically cross-link HA-aldehydes with PEG-bis(oxyamine), as the reaction is rapid and results in chemically stable gels.^{30,31} Oxidative cleavage is a common method to generate aldehydes from polysaccharides where the C–C bond between vicinal diols in the pyranose rings is cleaved and subsequent oxidation results in alcohols;^{27,32,33} however, undesired hydrolysis of the glycosidic bonds readily occurs, leading to HA backbone degradation, decreased molar mass, and inconsistent polymer syntheses. To overcome this limitation, we instead reacted HA carboxylic acids with amino acetaldehyde dimethyl acetal (an acid-labile protected aldehyde precursor)^{34,35} using 4-(4,6-dimethoxy-1,3,5-triazin-2-yl)-4-methylmorpholinium chloride (DMT-MM, Scheme 2) as a coupling agent. By controlling the molar equivalents of DMT-MM, HA was functionalized with the aldehyde precursor dimethyl acetal (HA-dma, 1) at 51 or 68% substitution (as determined by ¹H NMR, Figure 1 and Figure S1), which enables us to study the effect of aldehyde substitution on hydrogel properties.

Next, we independently control the biochemical properties by purposefully designing the HA hydrogels with a second bioorthogonal group, 5-methylfuran, which reacts with maleimide-functionalized peptides via Diels–Alder click chemistry. This strategy provides a distinct reaction from that used in chemical cross-linking, thereby providing independent control of mechanical and chemical properties. 5-Methylfurfurylamine is coupled to unreacted backbone carboxylic acids of HA-dma using DMT-MM, resulting in a bifunctional HA with a methylfuran substitution of 16% (HA-MF-dma, 2) (Figure 1). Dimethyl acetal protecting groups are completely cleaved under acidic conditions (aqueous 0.20 M hydrochloric acid at 20 °C for 24 h) generating HA substituted with both methylfuran and aldehyde (HA-MF-ald, 3). Aldehyde substitution was quantified using an established protocol,²⁷ where aldehydes on the HA-MF-ald backbone were reacted with *tert*-butoxycarbonyl hydrazide followed by sodium cyanoborohydride reduction (HA-MF-hydrazide(Boc), 4), yielding an aldehyde substitution of 51 or 68%, consistent with the DMA substitution of the HA-dma precursor (1). Importantly, and in contrast to previous reports of HA-aldehyde syntheses via oxidative cleavage,^{32,36} our chemical modification methodology resulted in only a 15% decrease in the HA weight-average molar mass, from M_w 330.1 to 284.1 kg mol⁻¹, as determined by GPC.

HA-MF-ald is air-stable following dissolution in aqueous medium and can be dissolved and stored as a stable and usable

Scheme 2. Synthesis of Bifunctional Hyaluronan (HA) with 5-Methylfuran and Aldehyde Functional Groups



solution for at least 3 months at 4 °C. In contrast, HyStem (comprising HA-thiol and gelatin-thiol) is susceptible to air oxidation after several days, resulting in undesired self-

polymerization after these components are dissolved in aqueous buffer. This inherently limits the reactivity of HA-thiol and gelatin-thiol with PEG diacrylate cross-linkers, leading to hydrogels with irreproducible physicochemical properties.

Having synthesized HA functionalized with both methyl furan and aldehyde motifs (HA-MF-ald) (3), hydrogels were formed with independent control of both chemical and mechanical properties. The hydrogel stiffness can be tuned by varying either the percent of aldehydes cross-linked with bis(oxyamine)-PEG (5) or the degree of aldehyde substitution (Figure 2). Using 1.1% bifunctional HA hydrogels with 51%

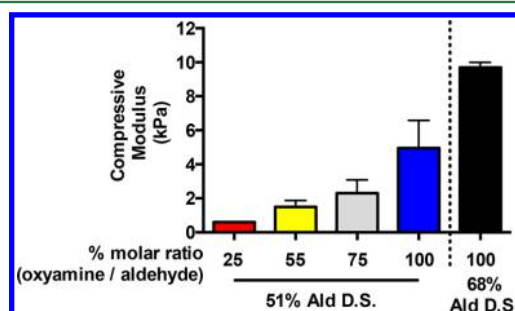


Figure 2. Compressive modulus of bifunctional 1.1% HA-MF-ald hydrogels with 51% degree of aldehyde substitution (except for last bar, black, at 68%) and cross-linked with bis(oxyamine)-PEG (25–100% molar ratio of oxyamine relative to aldehyde).

aldehyde substitution, the compressive modulus can be tuned from 0.60 ± 0.03 to 4.95 ± 1.64 kPa by increasing the molar ratio of oxyamine to aldehydes from 25 to 100%, respectively, with the conjugation efficiency of bis(oxyamine)-PEG being quantitative for the latter gels (Figure S9). In addition, increasing the aldehyde substitution from 51 to 68% further increases the modulus to 9.69 ± 0.31 kPa.

Next, pendant maleimide-functionalized peptides were chemically conjugated to the methylfuran groups of preformed bifunctional HA-MF-ald/PEG hydrogels (Figure 3A). Specifically, we conjugated a laminin $\alpha 1$ chain mimic, maleimide-

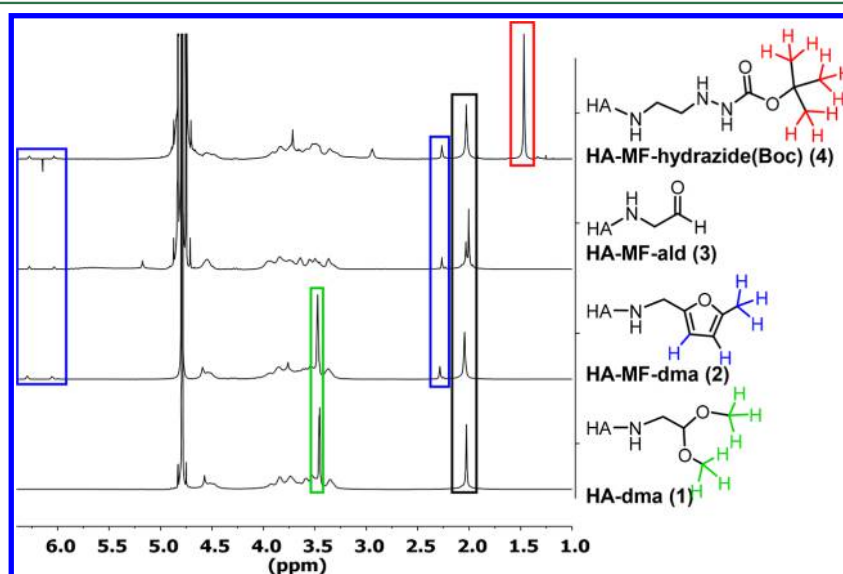


Figure 1. ^1H NMR spectra of 1–4. Highlighted proton peaks (in blue, green, and red boxes) were integrated relative to the *N*-acetyl signal of the HA backbone (2.1 ppm, black box) and used to quantify the degree of substitution of aldehydes (red) and methylfuran (blue). Detailed ^1H NMR spectra are shown in the Supporting Information.

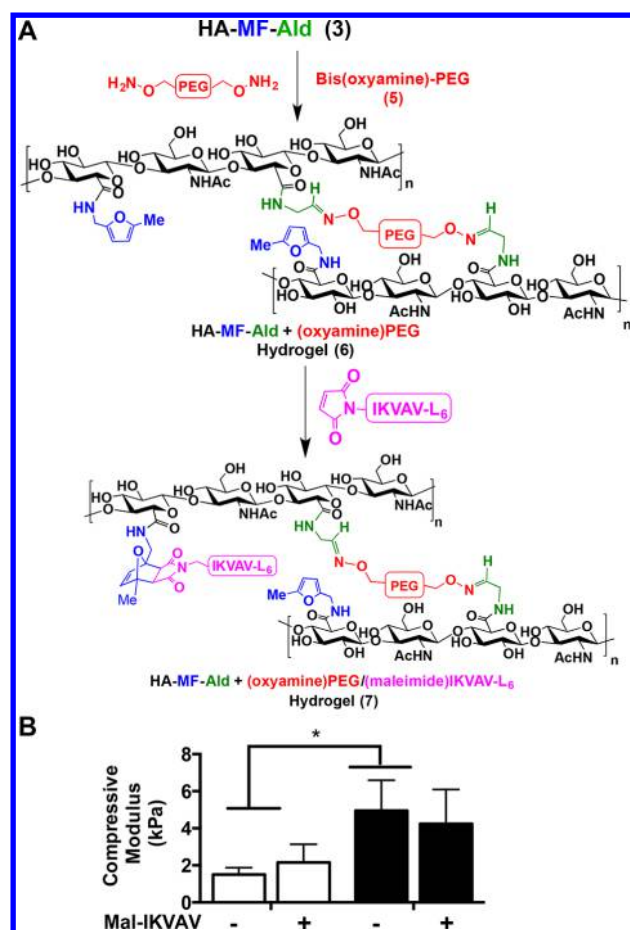


Figure 3. (A) Synthesis and (B) mechanical properties of hyaluronan-methylfuran-aldehyde (3, HA-MF-ald) hydrogels cross-linked with bis(oxyamine)-(PEG) (55% (open bars) or 100% (closed bars) molar ratio of oxyamine relative to aldehyde) and conjugated with Mal-IKVAV- L_6 peptide. Addition of peptide does not affect hydrogel stiffness. $N \geq 4$, mean + s.d. plotted. * $p < 0.05$. Two-way ANOVA, Tukey's post hoc test.

GRKQAAS-IKVAV-SG $_4$ SRL $_6$ R $_2$ KG (referred to as Mal-IKVAV- L_6),^{25,37} to promote the formation of breast cancer spheroids. We determined the peptide conjugation efficiency using amino acid analysis. When the same concentration of peptides (35 nmol/mg_{HA}) was added to gels with varying stiffness (0.6 or 1.6 kPa), the peptide conjugation efficiency was not statistically different ($73.7 \pm 10.6\%$ vs $57.1 \pm 11.7\%$, $p > 0.05$); however, peptide conjugation efficiency was significantly lower when the concentration of peptide was increased (from 35 to 75 nmol/mg_{HA}) in gels of the same stiffness (0.6 kPa) ($73.7 \pm 10.6\%$ vs $37.2 \pm 2.7\%$, $p < 0.01$) (Figure S10). The addition of peptides did not significantly change the stiffness of the bifunctional hydrogels (Figure 3B), indicating that the cross-linking chemistry was unaffected.

To demonstrate the advantage of using multiple functionalities to independently tune chemical and physical properties, we prepared 1.1% HA-methylfuran (6, HA-MF, 60% degree of substitution (D.S.), Figure 4A) and first cross-linked it with bis(maleimide)-PEG and then modified it with Mal-IKVAV- L_6 . In these hydrogels, the modulus decreased significantly after peptide modification even though it had already been cross-linked. In contrast, the incorporation of peptides did not affect the modulus of the hydrogels comprising both methyl furan and aldehyde functionalities that were cross-linked with

bis(oxyamine)-PEG and modified with the same Mal-IKVAV- L_6 peptide (Figure 4B).

To demonstrate the advantage of using multiple functionalities to independently tune chemical and physical properties, we prepared 1.1% HA-methylfuran (6, HA-MF, 60% degree of substitution (D.S.), Figure 4A) and first cross-linked it with bis(maleimide)-PEG and then modified it with Mal-IKVAV- L_6 . In these hydrogels, the modulus decreased significantly after peptide modification even though it had already been cross-linked. In contrast, the incorporation of peptides did not affect the modulus of the hydrogels comprising both methyl furan and aldehyde functionalities that were cross-linked with bis(oxyamine)-PEG and modified with the same Mal-IKVAV- L_6 peptide (Figure 4B).

To understand why the modulus decreased for HA-MF hydrogels cross-linked with (bis-maleimide)-PEG and then modified with Mal-IKVAV- L_6 peptide, we examined the mechanism. Given the reversibility of the Diels–Alder reaction,³⁸ we hypothesize that methylfuran groups of HA and maleimide groups of the PEG cross-linker are released from the Diels–Alder adduct. Reformation of chemical cross-links of maleimide-(PEG) with methyl furan groups of HA-MF is then competitively inhibited by addition of Mal-IKVAV- L_6 peptides, consequently decreasing the degree of chemical cross-linking and weakening the hydrogel (Figure 4C).

With our interest in developing bioengineered scaffolds for culturing breast cancer spheroids, we designed our hydrogel to mimic the physical properties of Matrigel, which is widely used to grow spheroids.^{3,6–8} The stiffness of bifunctional HA hydrogels, 0.60 ± 0.03 kPa, matched closely with Matrigel (0.98 ± 0.30 kPa) and HyStem (0.64 ± 0.15 kPa), another commercially available HA-based hydrogel. These bifunctional HA hydrogels are composed of 1.1% HA with a degree of substitution of 51% aldehyde and cross-linked with bis-(oxyamine)-PEG (25% molar ratio of oxyamine to aldehyde, Figure 5A). To further study the role of gel stiffness on spheroid formation, we also prepared a stiffer hydrogel (2.30 ± 0.79 kPa) by increasing the molar ratio of oxyamine to 75%.

Long-term cell culture (>28 d) is desirable for spheroid formation in vitro, drug screening, and genetic analysis of the cells. Using an in vitro swelling study of gels with comparable moduli, the stability of bifunctional HA-MF-ald/PEG gels with either low (25%) or high (75%) cross-linking was assessed. Bifunctional hydrogels were stable and showed no decrease in swelling ratio for at least 28 d, whereas HyStem and Matrigel showed significant decreases after 7–14 days (Figure 5B). Despite the increased stability of bifunctional HA-MF-ald/PEG gels, they remain degradable by hyaluronidase to enable retrieval of viable cells for further study.³⁹

Incorporation of both bioorthogonal functional groups on the same HA polymer backbone was important for gel stability. We performed a swelling study on hydrogels comprising a physical blend of each of these bioorthogonal functional groups on separate HA polymer backbones (i.e., HA-MF (6) + HA-ald (7)) vs HA-MF-ald (3), where all polymers were cross-linked with the same concentration of bis(oxyamine)-PEG (5). Unlike the bifunctional HA-MF-ald polymer (shown in Figure 5B), the physical blend of the separate HA-MF and HA-ald polymers resulted in a significantly greater swelling ratio and consequently decreased physical stability after 1 day, followed by mass loss (Figure S11). We attribute this decreased stability to the dissolution of HA-MF, which is not covalently cross-linked by bis(oxyamine)-PEG.

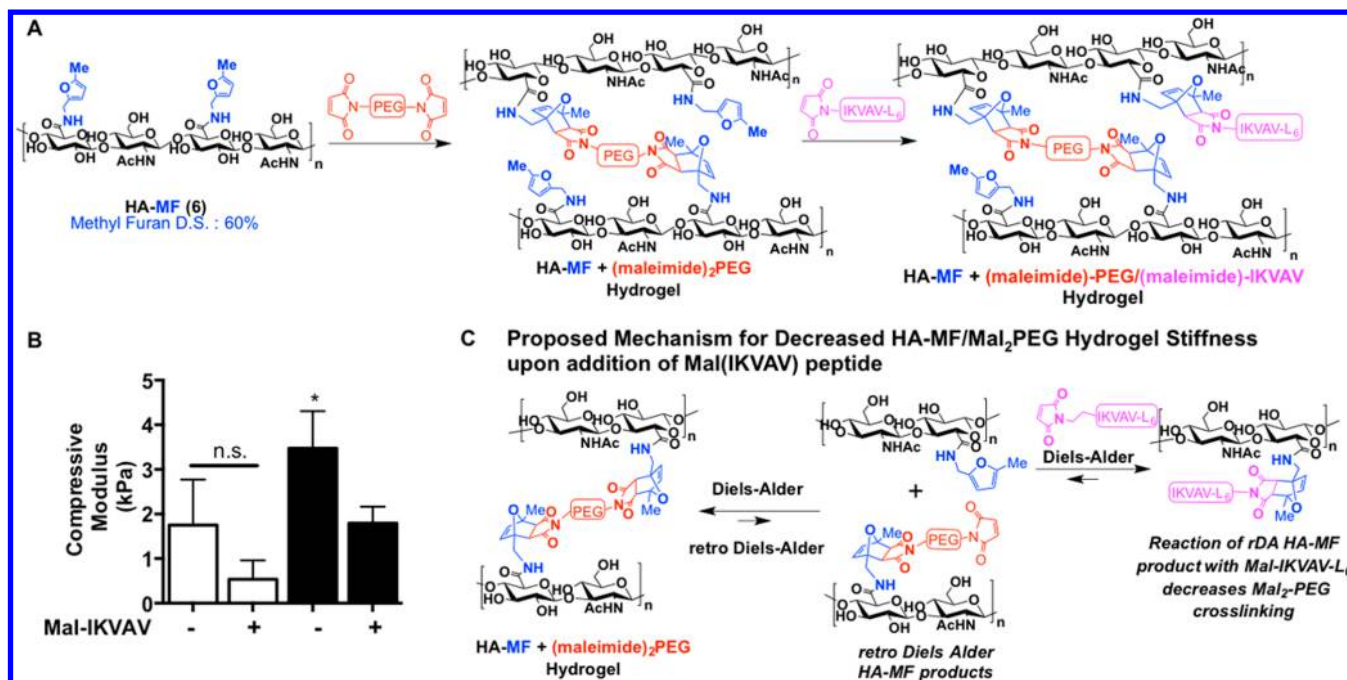


Figure 4. (A) Synthesis and (B) mechanical properties of hyaluronan-methylfuran (6, HA-MF) hydrogels cross-linked with bis(maleimide)-PEG (55% (open bars) or 100% (closed bars) molar ratio of maleimide relative to furan) decrease with Mal-IKVAV-L₆ peptide conjugation. Addition of peptide decreases the compressive modulus of the stiffer (100% cross-linked) HA-MF hydrogel. $N \geq 3$, mean + s.d. plotted. * $p < 0.05$. Two-way ANOVA, Tukey's post hoc test. (C) Proposed mechanism for decreased stiffness of HA-MF/Mal₂PEG hydrogels upon addition of Mal-IKVAV-L₆ peptide.

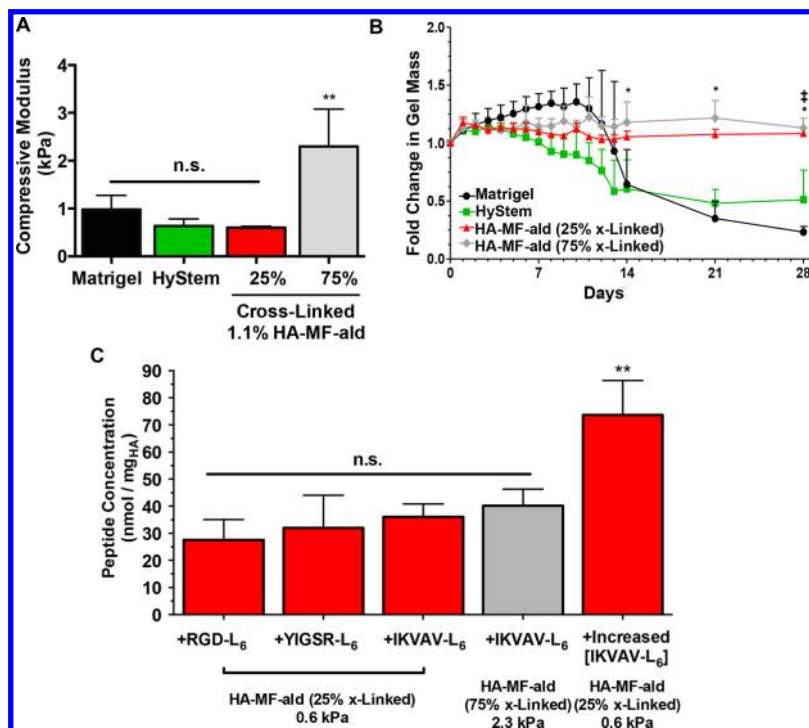


Figure 5. (A) Mechanical properties of Matrigel, HyStem, and 1.1% HA-MF-ald cross-linked with bis(oxyamine)-PEG (with 25% (red) or 75% (gray) molar ratios of oxyamine to aldehyde). (B) Swelling ratio shows improved HA-MF-ald/PEG gel stability at 28 d compared to those of Matrigel and HyStem. (C) Concentration of immobilized ECM-mimetic peptides to HA-MF-ald/PEG hydrogels quantified by amino acid analysis. For A,C: $N \geq 3$, mean + standard deviation plotted. ** $p < 0.01$; n.s. = not significant. One-way ANOVA, Tukey's post hoc test. For B: $N = 3$, student's t test was performed to evaluate differences in hydrogel swelling between materials at individual days. * $p < 0.05$ indicates the difference between bifunctional HA gels and Matrigel/HyStem; † $p < 0.05$ indicates difference between Matrigel and HyStem.

With similar mechanical properties to Matrigel, we screened HA-MF-ald/PEG with biochemical ligands for spheroid

growth. Given the complexity of the extracellular matrix (ECM), we introduced a series of peptides derived from

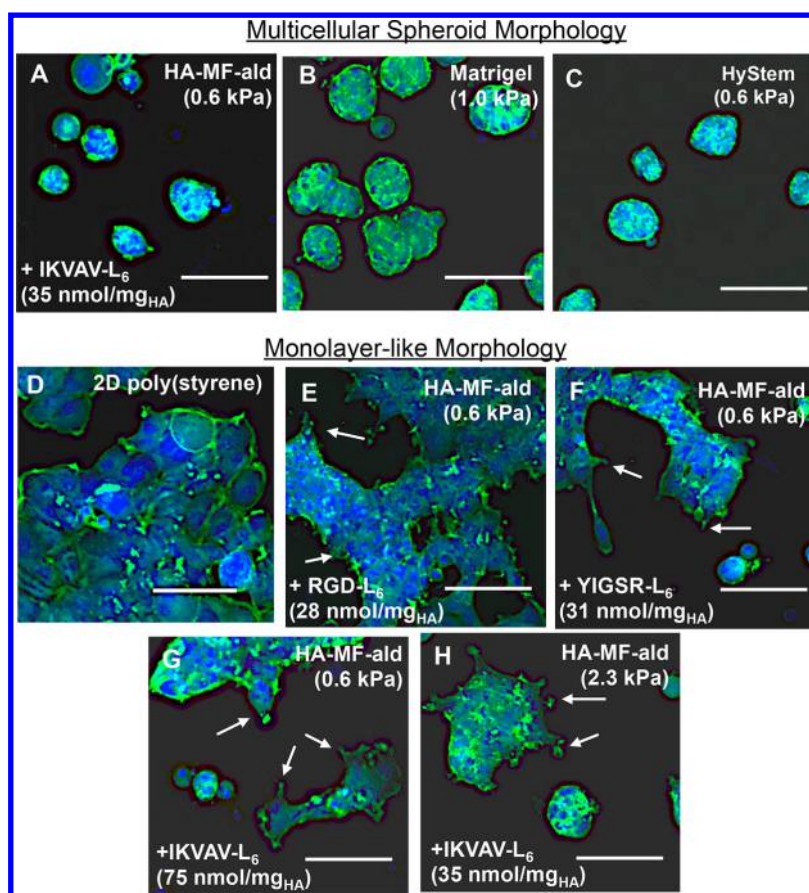


Figure 6. Cell morphology of T47D breast epithelial cancer cells cultured on (A) HA-MF-ald/PEG (0.6 kPa) with 35 nmol/mg_{HA} Mal-IKVAV-L₆, (B) Matrigel (positive control), (C) HyStem, (D) 2D TCPS (control), (E–G) HA-MF-ald/PEG (0.6 kPa) with (E) Mal-RGD-L₆ peptide, (F) Mal-YIGSR-L₆ peptide, and (G) increased concentrations of Mal-IKVAV-L₆ (75 nmol/mg_{HA}), (H) stiffer bifunctional HA-IKVAV-L₆ gels (2.3 kPa). Scale bar = 150 μm. Blue: Hoechst (nuclei), green: Phalloidin (Actin).

major ECM components that we could screen with a phenotype cell-based assay. Specifically, we conjugated maleimide-containing peptides derived either from fibronectin (G-RGD-SPASSK-G₄SRL₆R₂K₂-(maleimide)-G), laminin α 1 (Mal-IKVAV-L₆), or laminin β 1 (maleimide-GDPG-YIGSR-G₄SRL₆R₂KG) at similar peptide concentrations as determined by amino acid analysis (Figure 5C).²⁵

With the goal of identifying which hydrogel has the optimal biomimetic properties for breast cancer spheroids, we cultured luminal T47D breast epithelial cancer cells on HA-MF-ald/PEG hydrogels with varying mechanical properties and peptide compositions. We compared our HA-based hydrogels to both conventional 2D TCPS and commercially available hydrogels Matrigel and HyStem. Previous studies have shown the importance of adding a dilute, 2.5% solution of Matrigel to cells cultured on the surface of Matrigel to enable spheroid growth of breast epithelial cells.²⁹ Recognizing this, and along with our efforts to eliminate the use of Matrigel, we added a solution containing collagen IV, IKVAV-L₆, and YIGSR-L₆ peptides (at final concentrations of 20 μ g mL⁻¹, 20 μ M, and 1 μ M, respectively) to cells cultured on our bifunctional HA gels. Cells cultured on Matrigel with this protein/peptide cocktail showed equivalent cell morphology to those cultured with 2.5% Matrigel in solution (Figure S12A–D). Similarly, cells cultured on our bifunctional HA gels with the identical protein/peptide cocktail had a comparable morphology to those cultured on Matrigel (Figure S12E). Cells cultured in the

absence of these components in the media resulted in flattened cell morphologies or inconsistent spheroid growth (Figure S12F,G). Even with the protein/peptide cocktail in the media, cells cultured on HA bifunctional gels without immobilized IKVAV-L₆ peptide formed a nonadherent cell aggregate (Figure S12H).

Cells cultured on softer HA-MF-ald-IKVAV hydrogels (0.6 kPa), which have comparable compressive moduli to Matrigel and HyStem (1.0 and 0.6 kPa, respectively), formed spheroids (Figure 6A–C) on the surface of the hydrogels. In contrast, cells cultured on 2D TCPS grew as monolayers (Figure 6D), reflecting the inability of this conventional material to represent the cellular microenvironment. Although soft HA-MF-ald-IKVAV gels (0.6 kPa) were optimal for breast cancer spheroid formation, this was reproduced with neither HA-MF-ald-RGD nor HA-MF-ald-YIGSR with equivalent concentrations of immobilized peptide and compressive modulus, where T47D cells showed signs of a flattened morphology similar to that of 2D cultured cells (Figure 6E, F, white arrows). Peptide concentration also influenced cell fate as cells cultured on soft hydrogels (0.6 kPa) grafted with higher concentrations of IKVAV-L₆ peptides (75 nmol/mg_{HA}) formed regions with flattened cell morphology (Figure 6G, white arrows). In contrast, cells cultured in the absence of any immobilized peptides resulted in cells that adhered to each other and not to the gel, resulting in the formation of a large cell mass that was easily removed during the wash procedure (Figure S12H). The

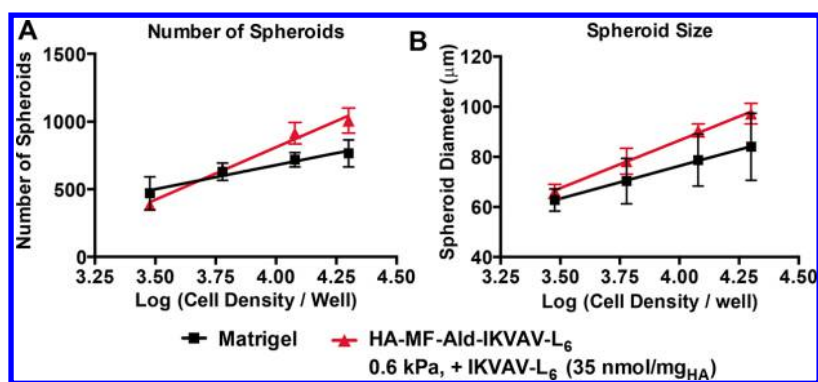


Figure 7. Effect of T47D cell seeding density on spheroid (A) number and (B) size on HA-MF-ald-IKVAV-L₆/PEG hydrogels (0.6 kPa, 35 nmol/mg_{HA} IKVAV-L₆) (red) or Matrigel (black) after 7 days of culture.

change in cell morphology as a function of peptide composition may be due to binding of specific types of cell-surface integrin receptors that cause specific downstream biochemical signaling to instruct cell growth.

To obtain greater insight into the role of mechanical properties on cellular spheroid culture, we took advantage of the versatility of our bifunctional HA gels and examined the role of gel stiffness. Cells cultured on stiffer HA-MF-ald/PEG gels (2.3 kPa, Figure 6H) with the optimal IKVAV peptide concentration of 35 nmol/mg_{HA} observed on softer HA gels showed that cell morphology changed from 3D spheroid structures (observed on 0.6 kPa gels, Figure 6A) to regions with flat monolayers (Figure 6H), corroborating previous reports that gel stiffness affects the morphology of breast epithelial cells.^{8,21,40} The change in cell morphology due to varying gel stiffness (with the same IKVAV-L₆ peptide concentration) suggests that complex cell–matrix interactions are occurring beyond integrin activation such as the regulation of cellular mechanotransduction pathways.

Notably, using HA-MF-ald-IKVAV gels, MCF-7 breast epithelial cancer cells were also cultured and formed multicellular 3D spheroids (Figure S13), thereby demonstrating the versatility of these well-defined, stable hydrogels for the culture of different cell types.^{8,21,40}

To gain an understanding of spheroid growth on bifunctional HA hydrogels, we first assessed cell viability after 7 days using a Live/Dead assay by staining with calcein AM (live cells, green) and ethidium bromide homodimer (dead cells, red), which showed comparable results to Matrigel (Figure S14). Cell growth after 7 days was further determined using a Presto Blue metabolic assay, which showed increased cell metabolism (suggesting increased cell numbers and therefore growth compared to those at day 1) when cells were cultured on our 3D bifunctional HA gels, Matrigel, and HyStem (Figure S15). Next, we compared spheroid number and size as a function of cell seeding density (Figure 7A, B) when cultured on bifunctional HA-MF-ald gels and Matrigel. After 7 days, the number of spheroids correlated with its initial cell density when cultured on either Matrigel or HA-MF-ald/PEG hydrogels with spheroid number exhibiting a greater dependence on initial cell density when cultured on HA-MF-ald/PEG hydrogels. Similarly, the average spheroid size is also correlated to initial cell density for cells cultured on either Matrigel or HA-MF-ald/PEG hydrogels, and importantly, these correlations (i.e., spheroid size on either material) were not significantly different from each other ($p = 0.187$). Our data suggest that HA-MF-ald/PEG hydrogels are comparable to Matrigel in enabling

breast cancer spheroid growth yet offer the advantages of being mechanically and chemically defined.

A goal of 3D cell culture is more predictive in vitro drug screening. A significant issue in discovering efficacious drug treatments for solid tumors is the inability for drugs to penetrate into the tumor mass and the development of drug resistance. Interior cells have reduced metabolism and proliferation, rendering them resistant to antiproliferative chemotherapeutic drugs.^{41,42} Moreover, larger spheroids limit the diffusion of drugs into their core.¹⁰ Although Matrigel is able to form spheroids that reflect their native cellular structures in vivo, the presence of undefined factors complicates drug screening. T47D breast cancer epithelial spheroids were cultured on either Matrigel or HA-MF-ald hydrogels for 7 days prior to treatment with varying concentrations of the clinical chemotherapeutic doxorubicin (Figure 8). Spheroids grown on Matrigel and treated with 0.05 μM doxorubicin or more for 7 days resulted in a shift in spheroid size distribution and decreased spheroid diameter (Figure 8A, B). However, higher (>0.1 μM) doxorubicin concentrations were required to decrease the size of spheroids cultured on HA-MF-ald (Figure 8C, D). To better understand these results, we imaged doxorubicin diffusion (which is intrinsically fluorescent) into spheroids of similar sizes cultured on Matrigel or HA-MF-ald hydrogels (Figure 7B). We observed increased drug penetration into T47D cells cultured on Matrigel (Figure 8E) than into spheroids cultured on bifunctional HA hydrogels (Figure 8F). For the latter, there was increased fluorescent signal at the exterior of the spheroids, suggesting that there is less drug penetration into breast cancer spheroids cultured on bifunctional HA gels (Figure S16).

Immunocytochemical staining of the multidrug resistant protein (MDR1) drug efflux pump (Figure 8G, H) revealed its upregulation in cells cultured in our HA gels but not in Matrigel. MDR1 is activated by CD44 binding, which is a native HA ligand, to pump out cytotoxic drugs such as doxorubicin and paclitaxel from the cell.⁴³ Surprisingly, MDR1 was not expressed in cells cultured in HyStem, another HA-based hydrogel (Figure S17), suggesting that our bifunctional HA-MF-ald hydrogel immobilized with IKVAV-L₆ peptides may be activating MDR1 by other mechanisms. Although several drug resistance mechanisms exist, these data demonstrate that our bifunctional HA gels provide an environment that better mimics this phenotype in vitro than both HyStem and Matrigel and are useful for screening drug targets that may generate drug resistance in cancer cells. This may in turn lead to more predictive drug screening.

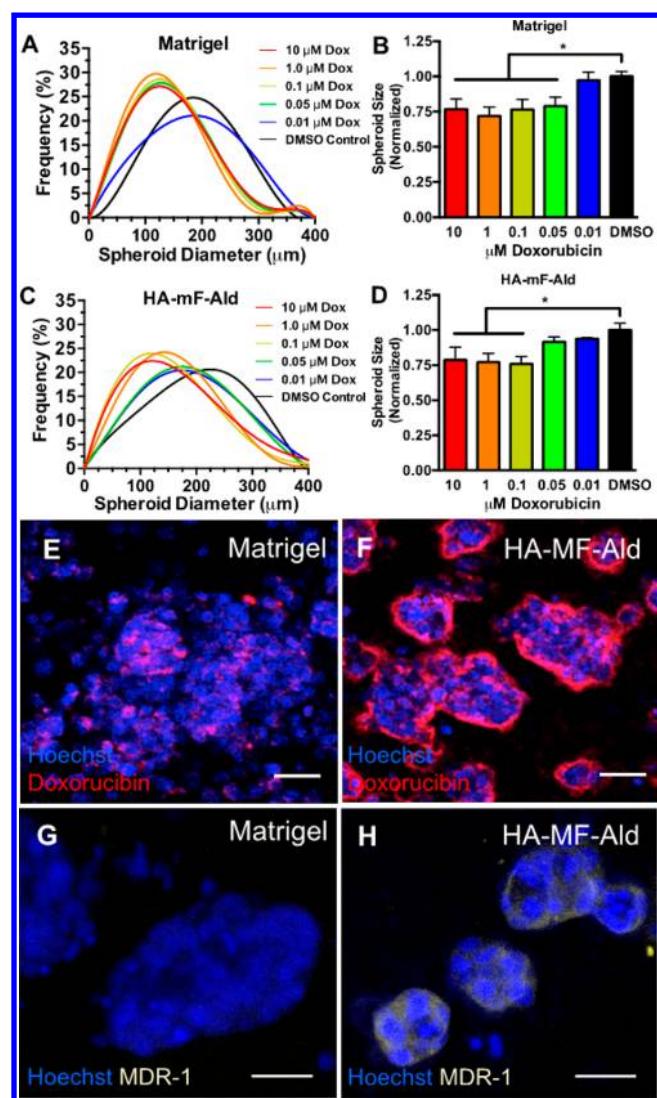


Figure 8. Treatment of T47D breast cancer spheroids cultured on (A, B) Matrigel or (C, D) HA-mF-Ald-IKVAV- L_6 gels with varying concentrations of Doxorubicin. (A, C) Fitted frequency distribution of spheroid sizes and (B, D) average spheroid diameter of spheroids formed on (A, B) Matrigel and (C, D) HA-mF-Ald-IKVAV- L_6 hydrogels. For B and D, $N = 3$ biological replicates, mean + s.d. * $p < 0.05$; (E, F) Distribution of doxorubicin (red) in cells (nuclei, blue, Hoechst), and (G, H) expression of multidrug resistance (MDR1) efflux pump (yellowish gray, anti-P glycoprotein antibody [EPR10364-57]) cultured on (E, G) Matrigel or (F, H) HA-mF-Ald-IKVAV- L_6 hydrogels. Scale bar = 50 μm .

CONCLUSIONS

In summary, the HA-MF-ald/PEG hydrogels designed herein allow two bioorthogonal “click” reactions for independent control of hydrogel stiffness and conjugation of peptide ligands. These new HA-based hydrogels, with an elastic modulus of approximately 0.6 kPa and laminin $\alpha 1$ -mimetic IKVAV peptides grafted therein, provide an optimal tissue mimetic scaffold for culturing T47D and MCF-7 breast epithelial cancer cells as 3D spheroids that resemble their in vivo morphology. T47D cells cultured on bifunctional HA hydrogels exhibited decreased doxorubicin penetration into the spheroid core and increased expression of the multidrug resistance protein MDR1, suggesting that cell culture in our bifunctional HA hydrogels will be useful for predictive drug screening.

ASSOCIATED CONTENT

Supporting Information

The Supporting Information is available free of charge on the ACS Publications website at DOI: 10.1021/acs.biomac.7b01422.

^1H NMR spectra, additional protocols for the synthesis of HA-MF and HA-ald, confocal images related to the screening of adhesive peptides, breast cancer growth, doxorubicin penetration, and MDR1 staining (PDF)

AUTHOR INFORMATION

Corresponding Author

*E-mail: Molly.Shoichet@utoronto.ca.

ORCID

Molly S. Shoichet: 0000-0003-1830-3475

Author Contributions

¹A.E.G.B. and R.Y.T. contributed equally to this work.

Notes

The authors declare no competing financial interest.

ACKNOWLEDGMENTS

We are grateful to the Canadian Institute of Health Research (CIHR) and Natural Sciences and Engineering Research Council of Canada (NSERC) and Pfizer Oncology for financial support through the Collaborative Health Research Program (to M.S.S.). A.E.G.B. acknowledges support from NSERC (PGSD) and Walter C Sumner Foundation Fellowship. We acknowledge the Canadian Foundation for Innovation, project number 19119, and the Ontario Research Fund for funding of the Centre for Spectroscopic Investigation of Complex Organic Molecules and Polymers. We thank members of the Shoichet Lab for thoughtful review of this paper, Dr. Senthil Muthuswamy (Harvard Medical School) for thoughtful discussions, and Professor Peter Zandstra (UofT) for use of his Celloomics instrument. We thank Laura Smith for the synthesis of monofunctional HA-methylfuran.

ABBREVIATIONS

HA, hyaluronan; MDR1, multidrug resistance protein 1; EHS, Engelbreth–Holm–Swarm

REFERENCES

- Zanoni, M.; Piccinini, F.; Arienti, C.; Zamagni, A.; Santi, S.; Polico, R.; Bevilacqua, A.; Tesei, A. 3D tumor spheroid models for in vitro therapeutic screening: a systematic approach to enhance the biological relevance of data obtained. *Sci. Rep.* **2016**, *6*, 19103.
- Rijal, G.; Li, W. 3D scaffolds in breast cancer research. *Biomaterials* **2016**, *81*, 135–56.
- Petersen, O. W.; Ronnov-Jessen, L.; Howlett, A. R.; Bissell, M. J. Interaction with basement membrane serves to rapidly distinguish growth and differentiation pattern of normal and malignant human breast epithelial cells. *Proc. Natl. Acad. Sci. U. S. A.* **1992**, *89*, 9064–9068.
- Fischbach, C.; Chen, R.; Matsumoto, T.; Schmelzle, T.; Brugge, J. S.; Polverini, P. J.; Mooney, D. J. Engineering tumors with 3D scaffolds. *Nat. Methods* **2007**, *4*, 855–60.
- Vinci, M.; Gowan, S.; Boxall, F.; Patterson, L.; Zimmermann, M.; Court, W.; Lomas, C.; Mendiola, M.; Hardisson, D.; Eccles, S. A. Advances in establishment and analysis of three-dimensional tumor spheroid-based functional assays for target validation and drug evaluation. *BMC Biol.* **2012**, *10*, 29.
- Debnath, J.; Brugge, J. S. Modelling glandular epithelial cancers in three-dimensional cultures. *Nat. Rev. Cancer* **2005**, *5*, 675–688.

- (7) Lama, R.; Zhang, L.; Naim, J. M.; Williams, J.; Zhou, A.; Su, B. Development, validation and pilot screening of an in vitro multicellular three-dimensional cancer spheroid assay for anti-cancer drug testing. *Bioorg. Med. Chem.* **2013**, *21*, 922–31.
- (8) Chaudhuri, O.; Koshy, S. T.; Branco da Cunha, C.; Shin, J.-W.; Verbeke, C. S.; Allison, K. H.; Mooney, D. J. Extracellular matrix stiffness and composition jointly regulate the induction of malignant phenotypes in mammary epithelium. *Nat. Mater.* **2014**, *13*, 970–978.
- (9) Vukicevic, S.; Kleinman, H. K.; Luyten, F. P.; Roberts, A. B.; Roche, N. S.; Reddi, A. H. Identification of multiple active growth factors in basement membrane Matrigel suggests caution in interpretation of cellular activity related to extracellular matrix components. *Exp. Cell Res.* **1992**, *202*, 1–8.
- (10) Lovitt, C. J.; Shelper, T. B.; Avery, V. M. Miniaturized three-dimensional cancer model for drug evaluation. *Assay Drug Dev. Technol.* **2013**, *11*, 435–48.
- (11) Benton, G.; Arnaoutova, I.; George, J.; Kleinman, H. K.; Koblinski, J. Matrigel: from discovery and ECM mimicry to assays and models for cancer research. *Adv. Drug Delivery Rev.* **2014**, *79–80*, 3–18.
- (12) Paszek, M. J.; Zahir, N.; Johnson, K. R.; Lakins, J. N.; Rozenberg, G. I.; Gefen, A.; Reinhart-King, C. A.; Margulies, S. S.; Dembo, M.; Boettiger, D.; Hammer, D. A.; Weaver, V. M. Tensional homeostasis and the malignant phenotype. *Cancer Cell* **2005**, *8*, 241–54.
- (13) Burdick, J. A.; Prestwich, G. D. Hyaluronic acid hydrogels for biomedical applications. *Adv. Mater. (Weinheim, Ger.)* **2011**, *23*, H41–56.
- (14) Kyburz, K. A.; Anseth, K. S. Synthetic mimics of the extracellular matrix: how simple is complex enough? *Ann. Biomed. Eng.* **2015**, *43*, 489–500.
- (15) Taubenberger, A. V.; Bray, L. J.; Haller, B.; Shaposhnikov, A.; Binner, M.; Freudenberg, U.; Guck, J.; Werner, C. 3D extracellular matrix interactions modulate tumour cell growth, invasion and angiogenesis in engineered tumour microenvironments. *Acta Biomater.* **2016**, *36*, 73–85.
- (16) Bohrer, L. R.; Chuntova, P.; Bade, L. K.; Beadnell, T. C.; Leon, R. P.; Brady, N. J.; Ryu, Y.; Goldberg, J. E.; Schmechel, S. C.; Koopmeiners, J. S.; McCarthy, J. B.; Schwertfeger, K. L. Activation of the FGFR-STAT3 pathway in breast cancer cells induces a hyaluronan-rich microenvironment that licenses tumor formation. *Cancer Res.* **2014**, *74*, 374–86.
- (17) Toole, B. P. Hyaluronan: from extracellular glue to pericellular cue. *Nat. Rev. Cancer* **2004**, *4*, 528–39.
- (18) Itano, N.; Sawai, T.; Miyaiishi, O.; Kimata, K. Relationship between hyaluronan production and metastatic potential of mouse mammary carcinoma cells. *Cancer research* **1999**, *59*, 2499–504.
- (19) Zhang, H.; Xu, X.; Gajewiak, J.; Tsukahara, R.; Fujiwara, Y.; Liu, J.; Fells, J. I.; Perygin, D.; Parrill, A. L.; Tigyi, G.; Prestwich, G. D. Dual activity lysophosphatidic acid receptor pan-antagonist/autotaxin inhibitor reduces breast cancer cell migration in vitro and causes tumor regression in vivo. *Cancer Res.* **2009**, *69*, 5441–9.
- (20) Fisher, S. A.; Anandakumaran, P. N.; Owen, S. C.; Shoichet, M. S. Tuning the Microenvironment: Click-Crosslinked Hyaluronic Acid-Based Hydrogels Provide a Platform for Studying Breast Cancer Cell Invasion. *Adv. Funct. Mater.* **2015**, *25*, 7163–7172.
- (21) Alcaraz, J.; Xu, R.; Mori, H.; Nelson, C. M.; Mroue, R.; Spencer, V. A.; Brownfield, D.; Radisky, D. C.; Bustamante, C.; Bissell, M. J. Laminin and biomimetic extracellular elasticity enhance functional differentiation in mammary epithelia. *EMBO J.* **2008**, *27*, 2829–2838.
- (22) Mbeunkui, F.; Johann, D. J. Cancer and the tumor microenvironment: a review of an essential relationship. *Cancer Chemother. Pharmacol.* **2009**, *63*, 571–582.
- (23) Schanté, C. E.; Zuber, G.; Herlin, C.; Vandamme, T. F. Chemical modifications of hyaluronic acid for the synthesis of derivatives for a broad range of biomedical applications. *Carbohydr. Polym.* **2011**, *85*, 469–489.
- (24) Zheng Shu, X.; Liu, Y.; Palumbo, F. S.; Luo, Y.; Prestwich, G. D. In situ crosslinkable hyaluronan hydrogels for tissue engineering. *Biomaterials* **2004**, *25*, 1339–48.
- (25) Tam, R. Y.; Fisher, S. A.; Baker, A. E. G.; Shoichet, M. S. Transparent Porous Polysaccharide Cryogels Provide Biochemically Defined, Biomimetic Matrices for Tunable 3D Cell Culture. *Chem. Mater.* **2016**, *28*, 3762–3770.
- (26) Owen, S. C.; Fisher, S. A.; Tam, R. Y.; Nimmo, C. M.; Shoichet, M. S. Hyaluronic Acid Click Hydrogels Emulate the Extracellular Matrix. *Langmuir* **2013**, *29*, 7393–7400.
- (27) Jia, X.; Burdick, J. A.; Kobler, J.; Clifton, R. J.; Rosowski, J. J.; Zeitel, S. M.; Langer, R. Synthesis and Characterization of in Situ Cross-Linkable Hyaluronic Acid-Based Hydrogels with Potential Application for Vocal Fold Regeneration. *Macromolecules* **2004**, *37*, 3239–3248.
- (28) Liu, Y.; Shu, X. Z.; Prestwich, G. D. Tumor engineering: orthotopic cancer models in mice using cell-loaded, injectable, cross-linked hyaluronan-derived hydrogels. *Tissue Eng.* **2007**, *13*, 1091–101.
- (29) Debnath, J.; Muthuswamy, S. K.; Brugge, J. S. Morphogenesis and oncogenesis of MCF-10A mammary epithelial acini grown in three-dimensional basement membrane cultures. *Methods* **2003**, *30*, 256–268.
- (30) Ulrich, S.; Boturyn, D.; Marra, A.; Renaudet, O.; Dumy, P. Oxime Ligation: A Chemospecific Click-Type Reaction for Accessing Multifunctional Biomolecular Constructs. *Chem. - Eur. J.* **2014**, *20*, 34–41.
- (31) Grover, G. N.; Lam, J.; Nguyen, T. H.; Segura, T.; Maynard, H. D. Biocompatible Hydrogels by Oxime Click Chemistry. *Biomacromolecules* **2012**, *13*, 3013–3017.
- (32) Sedova, P.; Buffa, R.; Kettou, S.; Huerta-Angeles, G.; Hermannova, M.; Leierova, V.; Smejkalova, D.; Moravcova, M.; Velebny, V. Preparation of hyaluronan polyaldehyde-a precursor of biopolymer conjugates. *Carbohydr. Res.* **2013**, *371*, 8–15.
- (33) Hardy, J. G.; Lin, P.; Schmidt, C. E. Biodegradable hydrogels composed of oxime crosslinked poly(ethylene glycol), hyaluronic acid and collagen: a tunable platform for soft tissue engineering. *J. Biomater. Sci., Polym. Ed.* **2015**, *26*, 143–61.
- (34) Bulpitt, P.; Aeschlimann, D. New strategy for chemical modification of hyaluronic acid: preparation of functionalized derivatives and their use in the formation of novel biocompatible hydrogels. *J. Biomed. Mater. Res.* **1999**, *47*, 152–69.
- (35) Bergman, K.; Engstrand, T.; Hilborn, J.; Ossipov, D.; Piskounova, S.; Bowden, T. Injectable cell-free template for bone-tissue formation. *J. Biomed. Mater. Res., Part A* **2009**, *91A*, 1111–1118.
- (36) Martinez-Ramos, C.; Lebourg, M. Three-dimensional constructs using hyaluronan cell carrier as a tool for the study of cancer stem cells. *J. Biomed. Mater. Res., Part B* **2015**, *103*, 1249–57.
- (37) Tashiro, K.; Sephel, G. C.; Weeks, B.; Sasaki, M.; Martin, G. R.; Kleinman, H. K.; Yamada, Y. A synthetic peptide containing the IKVAV sequence from the A chain of laminin mediates cell attachment, migration, and neurite outgrowth. *J. Biol. Chem.* **1989**, *264*, 16174–82.
- (38) Liu, Y.-L.; Chuo, T.-W. Self-healing polymers based on thermally reversible Diels-Alder chemistry. *Polym. Chem.* **2013**, *4*, 2194–2205.
- (39) Gerecht, S.; Burdick, J. A.; Ferreira, L. S.; Townsend, S. A.; Langer, R.; Vunjak-Novakovic, G. Hyaluronic acid hydrogel for controlled self-renewal and differentiation of human embryonic stem cells. *Proc. Natl. Acad. Sci. U. S. A.* **2007**, *104*, 11298–303.
- (40) Chatterjee, S.; Seifried, L.; Feigin, M. E.; Gibbons, D. L.; Scoppo, C.; Lin, W.; Rizvi, Z. H.; Lind, E.; Dissanayake, D.; Kurie, J.; Ohashi, P.; Muthuswamy, S. K. Dysregulation of cell polarity proteins synergize with oncogenes or the microenvironment to induce invasive behavior in epithelial cells. *PLoS One* **2012**, *7*, e34343.
- (41) Sutherland, R. M. Cell and environment interactions in tumor microregions: The multicell spheroid model. *Science* **1988**, *239*, 177–184.
- (42) Wenzel, C.; Riefke, B.; Grundemann, S.; Krebs, A.; Christian, S.; Prinz, F.; Osterland, M.; Golfier, S.; Rase, S.; Ansari, N.; Esner, M.;

Bickle, M.; Pampaloni, F.; Mattheyer, C.; Stelzer, E. H.; Parczyk, K.; Pechtl, S.; Steigemann, P. 3D high-content screening for the identification of compounds that target cells in dormant tumor spheroid regions. *Exp. Cell Res.* **2014**, *323*, 131–43.

(43) Bourguignon, L. Y. W.; Peyrollier, K.; Xia, W.; Gilad, E. Hyaluronan-CD44 Interaction Activates Stem Cell Marker Nanog, Stat-3-mediated MDR1 Gene Expression, and Ankyrin-regulated Multidrug Efflux in Breast and Ovarian Tumor Cells. *J. Biol. Chem.* **2008**, *283*, 17635–17651.